Transmembrane Domain Inversion Blocks ER Release and Insulin Receptor Signaling†

Kazunori Yamada,‡ Edison Goncalves,‡ Jean-Louis Carpentier,§ C. Ronald Kahn,‡ and Steven E. Shoelson*,‡

Joslin Diabetes Center and Department of Medicine, Harvard Medical School, Boston, Massachusetts 02215, and Department of Morphology, University of Geneva, 1211 Geneva 4, Switzerland

Received August 30, 1994; Revised Manuscript Received November 4, 1994®

ABSTRACT: Activation of the insulin receptor, like other tyrosine kinase receptors, appears to require dimerization. We have shown previously that, even in the absence of insulin, full receptor activation can be induced by changes in the receptor transmembrane domain (TMD), suggesting that TMD dimerization is sufficient for receptor activation. To further understand the importance of the TMD in insulin receptor activation, we have inverted the entire TMD sequence including flanking basic amino acids, residue-for-residue. This mutation was predicted to alter the ability of a TMD α-helix to form homodimers and higher level aggregates. Despite apparently normal protein folding on either side of the membrane, this mutation caused ER retention and, for those receptors that reached the cell surface, blockade of insulin-stimulated kinase signal transmission. However, the signaling blockade could be overcome by proteolytic activation with trypsin. In contrast, shifting only the basic cytoplasmic residues to the opposite side of the TMD or mutation to neutral residues had no detectable effect on assembly, biosynthesis, topology, or signaling. These findings extend our previous observations to suggest that TMD interactions within the membrane are not only sufficient for receptor activation, but may be required. TMD interactions also appear to be necessary for oligomeric assembly and biosynthetic maturation of the insulin receptor.

The insulin receptor is a tetrameric glycoprotein composed of two α- and two β-subunits, each with discrete functional domains. A single transmembrane domain (TMD) within each αβ-half receptor divides the receptor into extracellular and intracellular portions. Insulin binds to α-subunits outside the cell, whereas a tyrosine kinase domain and tyrosine phosphorylation sites are within the intracellular portions of the β-subunits. We have been interested in understanding on a molecular level how insulin binding activates the receptor kinase. It seems clear that insulin binding to the holoreceptor induces a conformational change which leads to the phosphorylation of one β-subunit by the other (Treadway et al., 1991; Fratalli et al., 1992). Moreover, selectively engineered changes in insulin receptor structure activate phosphorylation in an insulin-like fashion, including removal of the extracellular receptor (Shoelson et al., 1988; Ellis et al., 1987) and specific alterations in the TMD. In particular, the insulin receptor kinase is activated following substitution of its entire TMD with the corresponding domain of neu/erbB2 (Yamada et al., 1992; Cheatham et al., 1993).

neu/erbB2 is an EGF receptor-like proto-oncoprotein whose tissue levels are elevated in various malignancies (King et al., 1985). Chemically induced tumors in rats contain a specific point mutation in the neu/erbB2 TMD which leads to constitutive tyrosine kinase activation and increased transforming potential (Bargmann et al., 1986). Therefore, the TMD of neu/erbB2 has been the subject of considerable investigation and speculation (Bargmann et al., 1986; Bargmann & Weinberg, 1988; Weiner et al., 1989; Sternberg & Gullick, 1989; Cao et al., 1992; Gullick et al., 1992). Like most membrane-spanning motifs, the TMD of neu/erbB2 probably adopts an α-helical structure (Sternberg & Gullick, 1989; Gullick et al., 1992). Modeling studies suggest that the activating point mutations within the neu/erbB2 TMD induce helix homodimerization (Sternberg & Gullick, 1989). This model for neu/erbB2 activation is supported by findings in cells in which the mutated receptors aggregate in the absence of ligand similar to wild-type receptor aggregation following ligand binding (Weiner et al., 1989). These findings have also suggested that, for neu/erbB2, TMD interactions alone might be sufficient for kinase activation. By substituting the insulin receptor TMD with the corresponding domain of neu/erbB2 and showing that this resulted in full insulin receptor kinase activation, we further demonstrated that TMD interactions alone might be sufficient for activating the insulin receptor (Yamada et al., 1992; Cheatham et al., 1993).

These observations led us to hypothesize that TMD interactions might also occur during insulin-mediated activation of the wild-type receptor kinase and to wonder whether such interactions were required during normal signaling. The current studies were designed to test this possibility. Modeling studies suggest that inverting the sequence of an α-helix should alter its ability to form homodimers. In support of this design approach, the aggregation states of GCN4-related coiled coils were altered dramatically by inversion of hydrophobic residues within heptad repeats (Harbury et al., 1993). A reversal in α-helix orientation is conservative, in that all residues—hence net charge and hydrophobicity and their distributions—are identical. The potential for an inverted TMD sequence to form an α-helix is similar to that

† These studies were supported by Grants DK 43123, DK 31026, and DERC DK 36836 from the NIH, 31.34093.92 from the Swiss National Science Foundation, and the Juvenile Diabetes Foundation, International.

* To whom correspondence should be addressed at Joslin Diabetes Center, One Joslin Place, Boston, MA 02215. Phone: 617-732-2528. Fax: 617-732-2593. E-mail: shoelson@joslab.harvard.edu.

‡ Joslin Diabetes Center and Harvard Medical School.

§ University of Geneva.

® Abstract published in *Advance ACS Abstracts,* December 15, 1994.

0006-2960/95/0434-946$09.00/0

FIGURE 1: Mutagenesis of the insulin receptor stop-transfer (TM) domain. (A) Residues 913−944 (Ullrich et al., 1985) of the wild-type human insulin receptor. Hydrophobic, putative membrane-spanning residues are within the shaded box; basic residues are denoted by + markers. (B) The +exo/cyt mutation in which the Arg^{941}-Lys^{942}-Arg^{943} sequence is replaced by Gln-Asn-Gly. (C) The ++++exo/cyt mutation in which the three basic residues are moved from the cytoplasmic to exoplasmic sides of the transmembrane domain. (D) The ++++exo/+++cyt mutation with basic residues flanking both sides of the membrane. (E) The ST flip mutation in which the entire wild-type ST (TM) domain is inverted, residue-for-residue.

of the native TMD (Chou & Fasman, 1978), although N- and C-cap interactions (Richardson & Richardson, 1988) might be altered. We have inverted the orientation of the insulin receptor TMD within the intact receptor (Figure 1) and tested consequences on receptor signaling. The positions of flanking basic residues were altered as controls as well as to test whether interactions between these residues and membrane components might themselves influence receptor functioning.

MATERIALS AND METHODS

Recombinant DNA Techniques. cDNA sequences encoding mutated human insulin receptors were prepared by oligonucleotide-directed mutagenesis as previously described (Yamada et al., 1992; Goncalves et al., 1993). Synthetic oligonucleotides had the following sequences (mutated bases are underlined): +exo/cyt, 5′-TTT-ATC-TAT-TCC-CTG-GGA-AAT-GGG-CAG-CCA-GAT-GGG-CCG-3′; ++++exo/+++cyt, 5′-GTC-CCG-TCA-AGA-AAG-AGA-AAA-ATT-ATC-3′; flip, 5′-CCG-TCA-AAT-ATT-GCA-AAA-AGA-AAA-AGA-CTC-TTC-CTC-TAC-ATT-AGC-GGC-ATC-GTC-GTT-TCT-TTT-CTT-TTC-GTT-TTT-ATT-CTA-CCC-GGG-ATA-ATT-ATT-CAG-CCA-GAT-GGG-CCG-CTG-3′.

The +exo/cyt ($R^{941}K^{942}R^{943}$→QNG) and ++++exo/+++cyt ($N^{914}I^{915}A^{916}$→RKR) substitutions were created using either of the first two oligonucleotides independently, whereas the ++++exo/cyt substitution resulted from sequential use of both oligonucleotides (Figure 1). For the flip mutation the 114-base oligonucleotide was purified by HPLC prior to use (Yamada et al., 1992). Positive candidates were chosen by DNA sequencing the area of interest; selected clones were sequenced over the mutated region plus >50 bases upstream and downstream to confirm the absence of unexpected mutations. For the ++++exo/+++cyt receptor a second mutation was found in the kinase domain; therefore, subsequent use of this mutant was restricted to analyses of topology.

Cell Culture and Transfection. Monolayer Chinese hamster ovary (CHO) cells were grown in F-12 medium containing 10% fetal bovine serum (GIBCO). Cells were cotransfected with a neomycin resistance plasmid and the mutated human insulin receptor expression plasmids by calcium phosphate precipitation. Following transfection, cells were grown in the presence of 450 μg/mL Geneticin (GIBCO) to select for neomycin resistance. Transfected cells were separated by fluorescence-activated cell sorting (FACS) using a combination of human insulin receptor-specific monoclonal antibodies MAb 83-14 and MAb CT-1 (Prof. Ken Siddle of Cambridge University), which recognize extracellular and intracellular epitopes, respectively. Cells expressing the highest receptor numbers (upper 3−5%) were collected under sterile conditions for additional growth. Following 2−3 such passages, clonal cell lines expressing equivalent receptor numbers ($0.6-1.0 \times 10^6$ receptors/cell) were obtained by limiting dilution. Receptor densities for cells expressing flip receptors were substantially lower ($0.1-0.2 \times 10^6$ receptors/cells), even after six passages.

Biosynthetic Labeling of Cellular Proteins. Confluent monolayers of cell in 3.0 cm dishes were washed with methionine- and cysteine-free MEM media (Gibco) and incubated with the same media containing 0.5 mCi of [^{35}S]-methionine (New England Nuclear) for 20 min at 37 °C. Cells were washed and incubated (chased) with F-12 media supplemented with 2 mM methionine, 2 mM cysteine, and 5% fetal bovine serum. At the indicated times, media was removed and cells were solubilized with 50 mM Hepes buffer (pH 7.6) containing 1.0% Triton X-100, 2 mM PMSF, 10 μg/mL leupeptin, and 0.1 mg/mL aprotinin (solutilizing buffer). Labeled insulin receptors were immunoprecipitated with MAb 83-14, separated by SDS−PAGE, and identified by autoradiography.

Cell Solubilization and Receptor Isolation. Confluent cell monolayers were treated for 1 h with solubilizing solution (2 mL/15 cm dish) at 4 °C. Insoluble material was removed by centrifugation at 100000*g*, and supernatant solutions were passed over 1.0 mL columns of wheat germ agglutinin-agarose (WGA, Vector). The columns were washed extensively, and the partially purified receptors were eluted with 0.3 M *N*-acetylglucosamine in 50 mM Hepes and 0.1% Triton X-100, pH 7.6, and stored at −70 °C.

Insulin Binding Assays. Competitive binding analyses with [^{125}I]insulin and either intact cells or solubilized receptor preparations were as described (Yamada et al., 1992; Shoelson et al., 1992). Briefly, 24-well plates of confluent cells were washed to remove serum and incubated with 0.1 ng/mL [^{125}I]insulin and varying concentrations of unlabeled insulin in 0.5 mL/well of F-12 medium containing 10 mM HEPES and 0.1% bovine serum albumin (pH 7.6). Following a 5 h incubation at 15 °C, the cells were washed with ice-cold PBS (20 mM sodium phosphate, 0.14 M sodium chloride, pH 7.4) and lysed with a solution containing 0.1 N NaOH and 0.1% SDS. Binding assays with solubilized, WGA-purified receptors were performed at 4 °C for 18 h with 0.2 ng/mL [^{125}I]insulin and varying concentrations of unlabeled insulin in 0.2 mL of 50 mM HEPES, pH 7.6, containing 0.05% Triton X-100 and 0.1% bovine serum albumin. Receptor-associated radioactivity was precipitated with poly(ethylene glycol) in the presence of bovine γ-globulin (Shoelson et al., 1992).

Immunoblot Analyses. Solubilizing buffer (1.0 mL) was added to confluent cells in 10 cm dishes, resulting solutions were cleared by centrifugation, and receptor proteins were immunoprecipitated with MAb 83-14. Following separation by SDS−PAGE, proteins were transferred to nitrocellulose and detected by incubation with antireceptor antibody R1064, a conformation-insensitive, C-terminal β-subunit-directed antibody (kindly provided by Prof. Paul Pilch, Boston University), and [^{125}I]protein A, followed by autoradiography.

Cell Surface [^{125}I]Iodination. Confluent cells in 10 cm dishes were surface labeled by incubation with 0.1 mCi/mL [^{125}I]sodium iodide, 10 mM glucose, lactoperoxidase, and glucose oxidase as described (Backer et al., 1991). Cells were washed with PBS and treated with 1.0 mL/dish solubilizing solution. ^{125}I-Iodinated receptors were immunoprecipitated with MAb 83-14, separated by SDS−PAGE, and detected by autoradiography.

Immunofluorescence. To determine subcellular localization of the mutated insulin receptors, transfected cells were analyzed by fluorescence microscopy. Cells grown on microscope cover slips were washed five times with PBS at 4 °C, covered with acetone at −80 °C, and incubated for an additional 3 min at 20 °C. The acetone was removed, the cells were dried for 5 min, and PBS (4 °C) was added to the fixed and permeabilized cells. The cells were washed briefly with PBS (22 °C) and incubated with either anti-insulin receptor antibody (MAb 83-14) or antibodies directed against the endoplasmic reticulum protein, Bip (kindly provided by Dr. S. Fuller, EMBL, Heidelberg, Germany) or Golgi proteins (kindly provided by Dr. D. Louvard, Institut Pasteur, Paris, France) in PBS (22 °C) for 2 h. Following incubation with the first antibody, cells were washed with PBS, incubated with FITC-conjugated rabbit anti-mouse IgG (diluted 1:2000) for 1 h at 22 °C, rinsed with PBS, and counterstained with Evans blue. Cellular fluorescence patterns were determined using a Zeiss Axiophot microscope. Control experiments included incubations with second antibody only or an irrelevant first antibody.

Phosphorylation Reactions. Confluent cells in six-well plates were incubated with 100 nM insulin in serum-free F-12 medium at 37 °C for 5 min. Cells were washed with PBS, and reactions were terminated by addition of Laemmli sample buffer and heating to 100 °C. Phosphoproteins were separated by SDS−PAGE, transferred to nitrocellulose, and detected by blotting with anti-phosphotyrosine antibody and [^{125}I]protein A.

WGA-purified insulin receptor solutions were incubated 100 nM insulin in 50 mM Hepes (pH 7.6) containing 10 mM $MgCl_2$ and 5 mM $MnCl_2$ at 22 °C for 30 min. Kinase reactions were initiated by incubation with 100 μM [γ-^{32}P]-ATP at 22 °C and terminated after 10 min by addition of 1.0 mL of stopping solution (50 mM HEPES, 0.1% Triton X-100, 5 mM EDTA, 100 mM NaF, 20 mM sodium orthovanadate, and 2 mM sodium vanadate, pH 7.6). Insulin receptors were immunoprecipitated with MAb 83-14, separated by SDS−PAGE, and detected by autoradiography.

Tryptic Activation of Insulin Receptors. Similar amounts of WGA-purified insulin receptors (as determined by insulin binding studies) were incubated with 1.5 μM TPCK-treated trypsin in 50 mM HEPES, pH 7.6, for 1 or 3 min at 22 °C (Shoelson et al., 1988). Proteolysis reactions were stopped and kinase reactions initiated by addition of a solution containing 1 mg/mL aprotinin, 1 mM PMSF, 10 μg/mL leupeptin, 5 mM $MgCl_2$, and 100 μM [γ-^{32}P]ATP. Reactions were terminated by addition of Laemmli sample buffer, and proteins were separated by SDS−PAGE and detected by autoradiography.

RESULTS

Surface Topology of Mutant Insulin Receptors. Positions of basic residues and charge distribution surrounding membrane-spanning motifs dictate protein orientation within the membrane (von Heijne & Gavel, 1988; Hartmann et al., 1989; von Heijne, 1989; Boyd & Beckwith, 1990). Since the positions and distributions of basic residues surrounding the TMD of the insulin receptor (Figure 2) were intentionally altered, special care was taken to determine surface topology of the mutated receptors used in these studies. All receptors were recognized by MAb 83-14, an antibody directed against the α-subunit, whereas none were recognized by the intracellular β-subunit-directed antibody (Figure 3). Therefore, receptor topology was unaltered by deleting basic residues from the cytoplasmic face of the TMD (+exo/cyt), moving them to the opposite side of the TMD (++++exo/cyt), or placement at both sides of membrane (++++exo/+++cyt). The leftward shift in the Facs analyses of the flip receptor mutant, compared to wild-type or the other mutants, indicates a lower number of receptors at the cell surface, although their topology is normal.

Insulin Binding and Receptor Quantitation. Receptor numbers and insulin binding affinities were assessed with intact transfected cells as well as solubilized and WGA-purified receptor preparations (Figure 4 and Table 1). Receptor-binding affinities for all receptor types were indistinguishable, whether analyzed in intact cells (K_D = 0.7−1.2 nM) or solubilized extracts (K_D = 3.2−5.6 nM) (slightly higher affinities are typically observed when the same receptor type is analyzed in intact cells vs solubilized extracts). Receptor numbers were increased 30−50-fold for

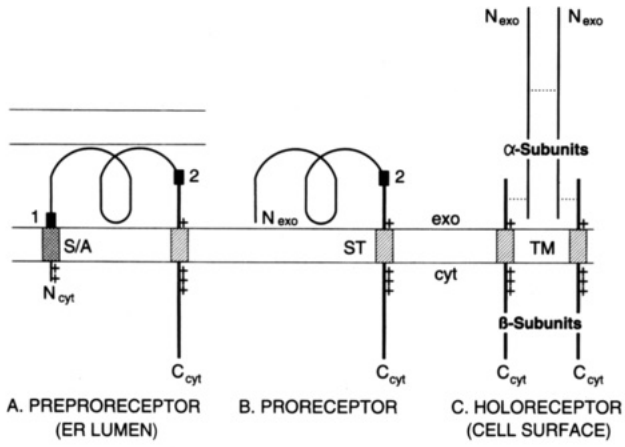

FIGURE 2: Schematic representation of insulin receptor biosynthesis. (A) Human insulin preproreceptor is synthesized as a single polypeptide chain, with its N-terminal signal/anchor (S/A) sequence fixed at the ER membrane in an N_{cyt} orientation. The growing peptide chain is translocated across the ER membrane until the stop-transfer (ST) sequence is reached, and the remainder of the newly translated peptide chain remains within the cytoplasm (C_{cyt}). Proteolytic cleavage within the ER lumen (solid box 1) yields the proreceptor (B) in its usual $N_{exo}C_{cyt}$ orientation. Subsequent proteolysis within a tetrabasic sequence (solid box 2), glycosylations, and cystine disulfide formation (dotted lines) result in generation of the intact $\alpha_2\beta_2$-holoreceptor (C). Note the "basics in" orientation of both signal/anchor and stop-transfer (TMD) sequences of the wild-type human insulin receptor.

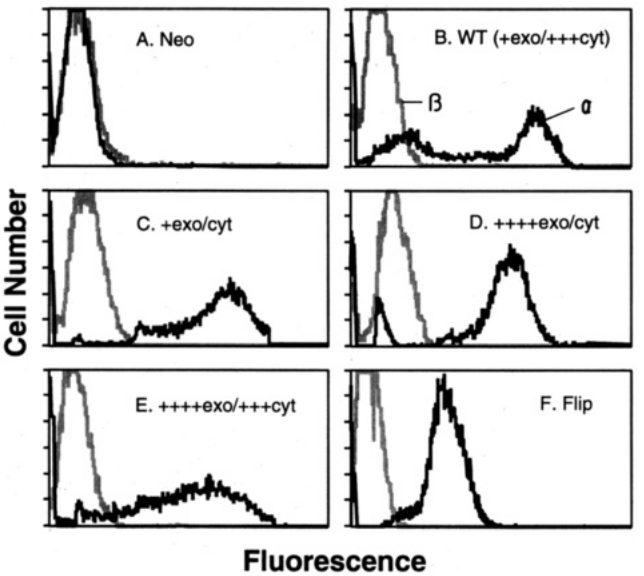

FIGURE 3: FACS analyses of transfected cells. Clonal cell lines expressing the neomycin resistance gene alone (A) and in combination with wild-type (B), +exo/cyt (C), ++++exo/cyt (D), ++++exo/+++cyt (E), and flip (F) insulin receptors were subjected to FACS analysis. Cells were incubated with antireceptor antibodies having specificity either for extracellular (black tracings; MAb 83-14) or intracellular (gray shaded tracings; MAb CT-1) determinants.

CHO cells transfected with wild-type (9.0×10^5/cell), +exo/cyt (6.2×10^5/cell), and ++++exo/cyt (9.6×10^5/cell) receptors, compared to the levels of endogenous hamster receptors (0.2×10^5/cell) (Table 1). Scatchard analyses with CHO cells transfected with flip receptors showed an intermediate number of cell surface receptors (1.4×10^5 receptors/cell), as compared to wild-type receptor- and mock-transfected (neo) cells (Figure 4). We conclude from the Scatchard analyses that binding affinities and stoichiometries for wild-type and mutated receptors are indistinguishable.

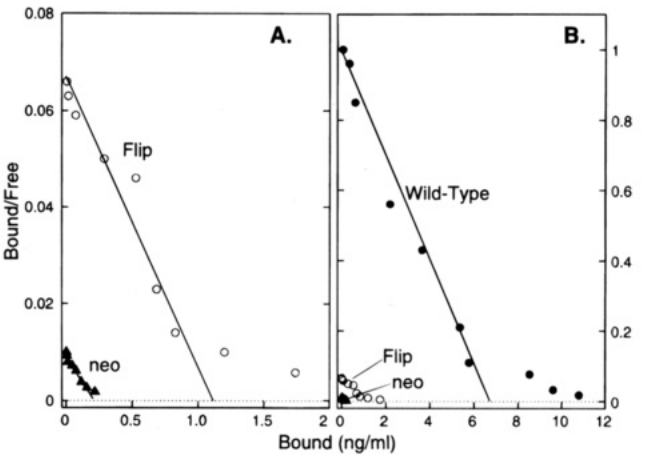

FIGURE 4: Insulin binding to transfected cells. Confluent 24-well plates of transfected cells were incubated with [^{125}I]insulin and varying concentrations of the unlabeled hormone. Following a 5 h incubation at 15 °C, the amounts of specifically associated insulin were used to generate Scatchard plots. The data for cells transfected with genes encoding neomycin resistance alone and flip receptors is displayed in panel A; data for the same cells and wild-type receptors is shown in panel B (note different scales). Calculated values of receptor number and affinity for all cell lines are tabulated in Table 1.

Table 1

	receptor number		affinity (nM)	
	intact cell ($\times 10^6$/cell)	WGA ($\times 10^{10}/\mu$L)	intact cell	WGA
wild-type	0.90	1.35	1.00	5.6
neo	0.02	0.02	1.20	4.5
+exo/cyt	0.62	3.53	0.80	5.0
++++exo/cyt	0.96	1.03	0.70	3.2
flip	0.14	0.17	0.74	3.7

Receptor numbers and gross structure were also analyzed by immunoblotting. The predominant receptor species present in cells transfected with wild-type receptors was the $\alpha_2\beta_2$ receptor, evidenced by the 95-kDa band detected by β-subunit directed antibody R1064 (Figure 5, lane 1). The 190-kDa proreceptor represents about 7% of the total receptor immunoreactivity (lane 1). Similar amounts of +exo/cyt and ++++exo/cyt receptor forms were detected in the corresponding transfected cells (Figure 5, lanes 2 and 3); no endogenous receptor was detected by these methods in neomycin-transfected cells (data not shown). As anticipated from insulin binding analyses, significantly less mature receptor (β-subunit) was detected in cells transfected with the flip receptor. However, in this case a large amount of 190-kDa proreceptor was present, accounting for 90% of the detected insulin receptor species (Figure 5, lane 4). Similar results were obtained with three distinct clones of wild-type and flip receptors (data not shown). These findings suggest that although an abundant quantity of flip proreceptor was synthesized, much was not processed into mature receptor.

Biosynthetic Labeling. Pulse−chase studies were used to look more directly at insulin receptor processing. Biosynthesis of the wild-type insulin receptor in transfected CHO cells proceeds normally, with initial generation of a 190-kDa proreceptor (Figure 6A, lane 1) and subsequent proteolytic processing into 135-kDa α- and 95-kDa β-subunits (lane 5). Biosynthesis and subunit sizes of the ++++exo/cyt and +exo/cyt mutant receptors appeared normal by these criteria (Figure 6A, lanes 2, 3, 6, and 7). By contrast, analyses of flip receptor biosynthesis showed production of

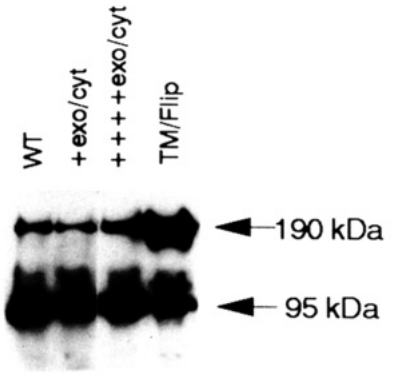

FIGURE 5: Receptor quantitation by immunoblotting. Confluent cells were solubilized with Triton X-100. Receptors were immunoprecipitated with MAb 83-14 anti-receptor antibodies, separated by SDS−PAGE, transferred to nitrocellulose, and detected with antibody R1064 (directed against the insulin receptor β-subunit) and [^{125}I]protein A. The insulin proreceptor and β-subunit are detected at 190 and 95 kDa, respectively.

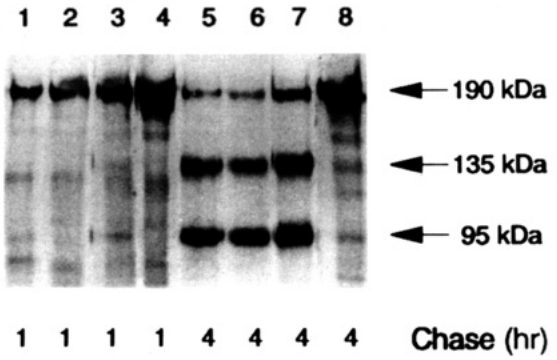

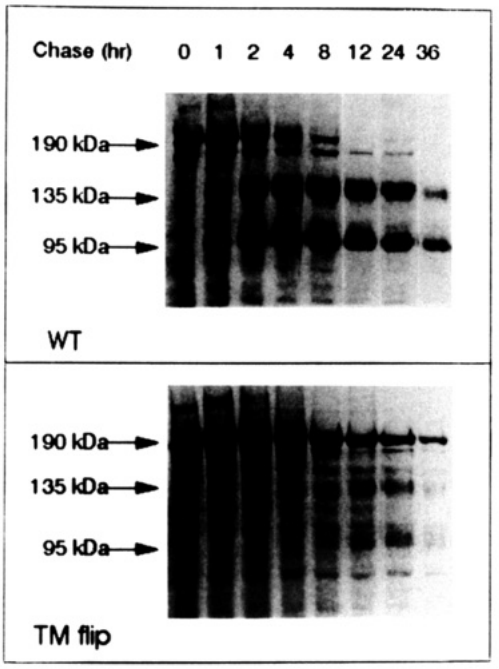

FIGURE 6: Pulse−chase experiments. (A, top) Cells expressing wild-type (lanes 1 and 5), +exo/cyt (lanes 2 and 6), ++++exo/cyt (lanes 3 and 7), and flip (lanes 4 and 8) insulin receptors were metabolically labeled with [^{35}S]methionine and [^{35}S]cysteine. Cells were then washed and chased with unlabeled methionine and cysteine for 1 h (lanes 1−4) or 4 h (lanes 5−8) and solubilized. Proteins were immunoprecipitated with anti-insulin receptor antibody, separated by SDS−PAGE, and detected by autoradiography. Insulin proreceptors (190 kDa) and α- (135 kDa) and β-subunits (95 kDa) are indicated with arrows. (B, bottom) Cells expressing wild-type (upper panel) and flip receptors (lower panel) were analyzed at additional chase times following similar methods.

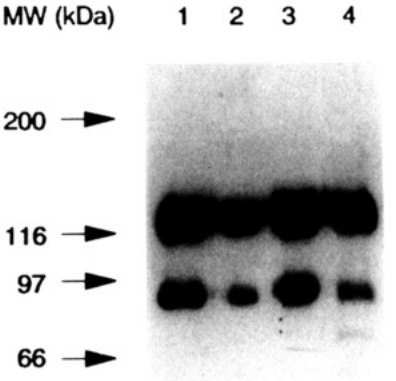

FIGURE 7: Labeling of cell surface proteins. Intact cells expressing wild-type (lane 1), +exo/cyt (lane 2), ++++exo/cyt (lane 3), and flip receptors (lane 4) were radiolabeled with [^{125}I]sodium iodide and lactoperoxidase as described in Materials and Methods. Cells were solubilized and labeled proteins were immunoprecipitated with anti-insulin receptor antibody MAb 83-14, separated by SDS−PAGE, and detected by autoradiography. A 10-fold greater volume of flip cell lysate was used for this analysis.

a proreceptor that was slightly smaller than the mature wild-type proreceptor (Figure 6), due to differences in oligosaccharide side chains (data not shown), and a striking reduction in the rate of proteolytic processing into α- and β-subunits (Figure 6A, lanes 4 and 8). In a more extended time course (Figure 6B), the flip proreceptor persisted even at 36 h postpulse and much less proreceptor conversion was observed, although low levels of α- and β-subunits were clearly present at longer pulse times (8−24 h). From these experiments we concluded that the processing of the flip proreceptor into $\alpha_2\beta_2$ holoreceptors was significantly delayed.

Labeling of Cell Surface Proteins. Cell surface proteins were labeled with [^{125}I]iodide to determine whether proreceptor forms were present at the cell surface. Both α- and β-subunits of wild-type receptors were labeled, with $\approx$80% of the incorporated radioactivity in the α-subunit (Figure 7, lane 1). Similar patterns and proportions were observed for +exo/cyt, ++++exo/cyt, and flip receptors (lanes 2, 3, and 4, respectively). Notably, although proreceptor forms can be immunoprecipitated with MAb 83-14 (e.g., Figures 5 and 6), no 190-kDa proteins were identified at the cell surface. These results suggest that the large amounts of flip proreceptors were present primarily inside the cell.

Fluorescence Microscopy. Fluorescence microscopy was used to localize receptor forms within subcellular compartments. CHO cells transfected with wild-type human insulin receptors and analyzed with human insulin receptor-specific MAb 83-14 showed a pattern of fluorescence nearly exclusively at the cell surface (Figure 8). By contrast, cells transfected with the flip receptor and similarly labeled show a reticular pattern for fluorescence throughout the cytoplasm, consistent with accumulation of the receptor in the ER. For a more precise comparative localization, cells were analyzed with antibodies directed against Golgi proteins and Bip, an ER-specific protein. The anti-Bip fluorescence showed a reticular pattern similar to that of the anti-insulin receptor antibody. Specific fluorescence patterns were not observed when transfected cells were incubated with or without irrelevant first antibody or when mock-transfected cells were analyzed with specific antibodies (data not shown). Therefore, the majority of flip receptor which was synthesized in the ER failed to exit. Proteolytic processing of the proreceptor normally occurs in the Golgi apparatus (Olson et

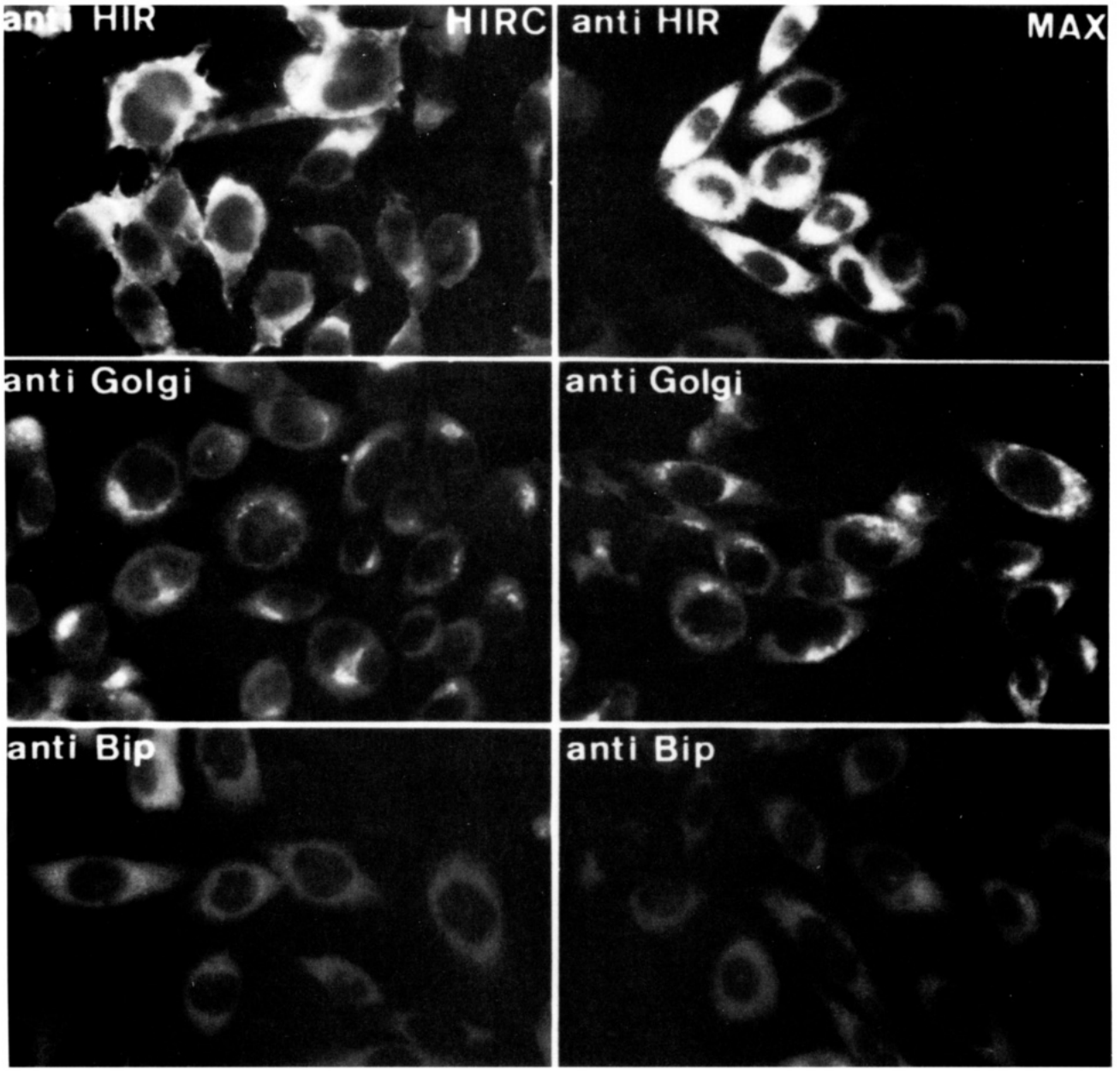

FIGURE 8: Immunofluorescence microscopy. Cells transfected with wild-type (left three panels) or flip (right three panels) receptors were treated first with anti-insulin receptor MAb (83-14) (top two panels), an anti-Golgi protein antibody (middle two panels), or anti-ER protein Bip antibody (lower two panels), and second with FITC-conjugated anti-mouse antibody. Note cell surface labeling of wild-type receptors (upper left) vs the reticular pattern observed for flip receptors (upper right). Proteins in the ER exhibit a reticular pattern (lower two panels).

al., 1988), and proreceptors that are trapped in the ER remain unprocessed.

Insulin Receptor Autophosphorylation and Substrate Kinase Activity. The abilities of mutated receptors to transmit insulin binding signals were assessed in intact cells and solubilized receptor preparations. Insulin-stimulated receptor autophosphorylation and endogenous substrate phosphorylation were assessed in intact cells by immunoblotting with anti-phosphotyrosine antibodies (Figure 9A). Mutated +exo/cyt (lanes 3 and 4) and ++++exo/cyt (lanes 5 and 6) receptors signaled normally, compared to wild-type receptor controls (lanes 1 and 2). In contrast, flip receptors showed no insulin-stimulated autokinase activity (lanes 7 and 8) over that produced by the endogenous hamster receptors (lanes 9 and 10). The same was true even when 5-fold greater numbers of flip-expressing cells were analyzed, as compared to wild-type controls.

Related experiments were conducted with solubilized, partially purified receptors (Figure 9B). Again, +exo/cyt (lanes 3 and 4) and ++++exo/cyt (lanes 5 and 6) receptors were found to signal normally, as compared to wild-type receptor controls (lanes 1 and 2), with ≈20-fold stimulation of autophosphorylation over basal. In contrast, phosphorylation observed in WGA-purified extracts from cells expressing flip receptors exhibited only ≈1.5-fold stimulation over basal (lanes 7 and 8). Similar phosphorylation patterns were observed for β-subunits (95 kDa) and unprocessed proreceptor (190 kDa). Results from exogenous substrate kinase assays (Yamada et al., 1992) paralleled the autophosphorylation (data not shown). Therefore, both *in vitro* and *in situ* insulin-stimulated autokinase and substrate kinase activities were severely impaired for flip receptors.

Tryptic Activation of Receptor Autokinase Activity. We have shown previously (Shoelson et al., 1988) that *in vitro*

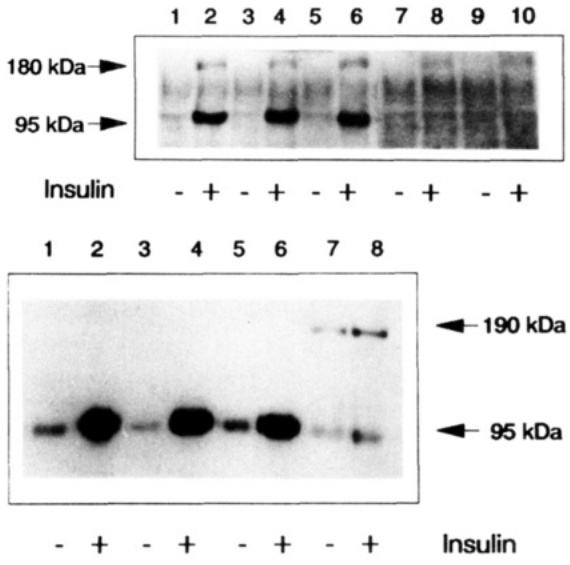

FIGURE 9: Phosphorylation reactions with intact cells and solubilized receptors. (A, top) Cells transfected with wild-type (lanes 1 and 2), +exo/cyt (lanes 3 and 4), ++++exo/cyt (lanes 5 and 6), and flip (lanes 7 and 8) receptor cDNA and the neomycin resistance gene alone (lanes 9 and 10) were stimulated (lanes 2, 4, 6, 8, and 10) or not (lanes 1, 3, 5, 7, and 9) with 100 nM insulin. Cells were lysed and proteins were separated by SDS−PAGE and detected by immunoblotting with anti-phosphotyrosine antibodies. The 95- and 180-kDa bands represent insulin receptor β-subunits and IRS-1, respectively. (B, bottom) WGA-purified wild-type (lanes 1 and 2), +exo/cyt (lanes 3 and 4), ++++exo/cyt (lanes 5 and 6), and flip (lanes 7 and 8) receptor preparations were treated with (lanes 2, 4, 6, and 8) or without (lanes 1, 3, 5, and 7) insulin. Proteins were phosphorylated with [γ-^{32}P]ATP, immunoprecipitated with anti-insulin receptor antibody MAb 83-14, separated by SDS−PAGE, and detected by autoradiography. The 95- and 190-kDa bands represent insulin receptor β-subunits and proreceptors, respectively.

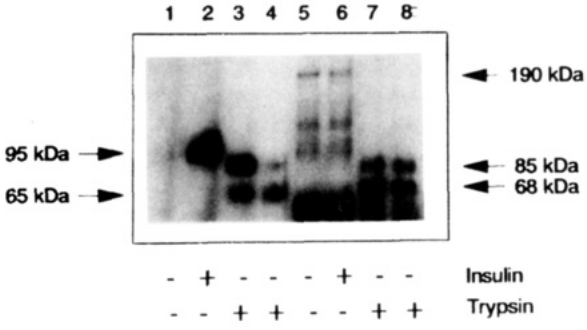

FIGURE 10: Tryptic activation of insulin receptor phosphorylation. Equivalent amounts of WGA-purified wild-type (lanes 1−4) or flip (lanes 5−8) insulin receptors were untreated (lanes 1 and 5) or treated with 100 nM insulin for 30 min (lanes 2 and 6) or 1.5 μM trypsin for 1 min (lanes 3 and 7) or 3 min (lanes 4 and 8). Proteins were phosphorylated with [γ-^{32}P]ATP in the presence of protease inhibitors, separated by SDS−PAGE, and detected by autoradiography. The 95- and 190-kDa bands represent intact insulin receptor β-subunits and proreceptors, respectively; 65-, 68-, and 85-kDa bands represent trypsin-activated receptor forms (Shoelson et al., 1988).

trypsin cleaves the wild-type receptor within the α- (Arg^{576}-Arg^{577}) and β-subunits ($Lys^{1313}Arg^{1314}$) to generate a kinase-active fragment (Figure 10, lanes 1 and 3). Although insulin does not activate the flip receptor kinase (lanes 5 and 6), when flip receptors were treated with trypsin, there was clear stimulation of autokinase activity (lanes 7 and 8). For the wild-type receptor an 85-kDa trypsin-activated β-subunit fragment was observed (Figure 10, lanes 1 and 3), as compared to the insulin-activated intact 95-kDa β-subunit (lane 2). Further proteolysis at the intracellular TMD boundary ($Arg^{941}Lys^{942}Arg^{943}$) resulted in formation of an additional 65-kDa fragment (lanes 3 and 4) which also possessed autokinase activity. The sizes of the 85-kDa fragments derived from wild-type and flip receptors were similar (reflecting proteolysis at the $Lys^{1313}Arg^{1314}$ site), whereas more extensive proteolysis of the flip receptor led to a slightly larger 68-kDa second fragment (lanes 7 and 8). This difference presumably results directly from the flip mutation. In reversing TMD orientation, the Arg-Lys-Arg sequence was moved to the opposite side of the flip TMD (Figure 1). Proteolysis at the new tetrabasic site results in a kinase-active fragment having 23 additional residues, which accounts for a difference in molecular mass of $\approx$3 kDa following SDS−PAGE. These studies verify that the kinase domain is functional and that the inability of insulin to stimulate flip receptor kinase activity results directly from a blockade between functional domains.

DISCUSSION

Cell surface receptors with intrinsic tyrosine kinase activity all have a similar molecular architecture: an extracellular, glycosylated ligand binding domain and a cytoplasmic domain with tyrosine kinase catalytic activity connected by a single TMD. The molecular mechanisms used by tyrosine kinase receptors for translating a ligand binding signal into tyrosine kinase domain activation are also similar and appear to be dictated both by the thermodynamic constraints of getting a signal across a membrane and the architecture of these receptors. Extracellular ligand binding induces receptor homodimerization. This in turn brings cytoplasmic tyrosine kinase domains into juxtaposition and facilitates phosphorylation of one cytoplasmic domain by another (Ullrich & Schlessinger, 1990). Although the heterotetrameric structure of the insulin receptor represents a variation on this architectural theme, with disulfide linkages between two $\alpha\beta$-half receptors, the mechanism of insulin-mediated receptor activation is similar. For example, the $\alpha_2\beta_2$-holoreceptor can be separated by limited reduction into kinase-inactive $\alpha\beta$-half receptors (Sweet et al., 1987; Boni-Schnetzler et al., 1988). Addition of insulin to purified half-receptors facilitates proper reassembly and restores kinase activation.

Additional observations suggest a common mechanism for class I (e.g., EGF, neu/erbB2) and class II (e.g., insulin) tyrosine kinase receptor activation (Ullrich & Schlessinger, 1990). First, elimination of the extracellular ligand-binding domain of the insulin receptor leads to constitutive activation of the β-subunit kinase (Shoelson et al., 1988; Ellis et al., 1987), similar to the relationship between erbB, a viral transforming protein with autonomous kinase activity, and the TGFα/EGF receptor (Downward et al., 1984). Secondly, substitution of the insulin receptor TMD with the corresponding domain of neu/erbB2 poises the insulin receptor kinase to be activated (Yamada et al., 1992), and the same point mutation within the TMD which activates neu/erbB2 itself (Bargmann et al., 1986) also activates the mutated insulin receptor (Cheatham et al., 1993). A model for receptor tyrosine kinase activation is suggested by these findings. In the unliganded state, the ligand binding domain prevents interactions between cytoplasmic domains; ligand binding leads to a conformational change which facilitates kinase domain interactions and phosphorylation. Physical removal of the ligand binding domain similarly relieves the inhibitory effect of the ligand binding domain to facilitate

kinase activation. Moreover, specific substitutions within tyrosine kinase receptor TMDs which appear to force homodimerization at the level of the TMD also facilitate kinase activation, thus bypassing the need for ligand.

Since TMD-mediated interactions in mutated receptors are sufficient for activating tyrosine kinase receptors, we have hypothesized that TMDs in wild-type receptors might also interact with one another during ligand stimulated activation, and that such interactions might be necessary during normal stimulation. A mutation which would block interactions between adjacent TMDs was needed to test this hypothesis. In the design of such a mutation it would be useful to know the rotational orientation of each TMD with respect to its parallel partner. As this information is unknown, we have attempted to develop a more general strategy for altering the aggregation state of interactive α-helices. Modeling studies suggested that sequence inversion would disturb interhelix interactions. This change is conservative in that all amino acids, and therefore charge and hydrophobicity, remain identical. A related approach has shown that for coiled coil interactions site-specific inversions within heptad repeats dramatically alters aggregation state (Harbury et al., 1993). To test these concepts, we have inverted the entire TMD of the wild-type insulin receptor, residue-for-residue, including the three basic residues which normally flank the TMD at its cytoplasmic surface, and these receptors were expressed stably in CHO cells. Repeated attempts to express receptors containing the inverted TMD alone (without basic residues) were unsuccessful. As controls, the three basic residues at the cytoplasmic side of the wild-type TMD (+exo/+++cyt) were changed to neutral residues (+exo/cyt) or moved to the opposite side of the membrane (++++exo/cyt).

Since altering the charge around and the sequence within a TMD might influence such diverse functions as membrane topology and anchoring, and protein biosynthesis and processing, in addition to transmembrane signaling, these processes were evaluated during characterization of the transfected cell lines. If a tribasic sequence at the cytoplasmic side of the TMD was necessary for signaling stop-transfer during biosynthesis within the ER (Figure 2), then elimination of the basic residues should allow the entire preproreceptor to be extruded into the ER lumen, and, following preproprotein proteolysis, the protein would be secreted. This does not occur. The +exo/cyt, ++++exo/cyt, and flip receptor forms all remain anchored at the cell membrane. In addition, we have failed to find secreted receptor in the media removed from cultured cells, using [^{35}S]metabolic labeling and immunoprecipitation (data not shown). Therefore, stop-transfer of the nascent chain is signaled and anchoring appears to be normal, either in the absence of cytoplasmic basic residues or when inappropriately placed, indicating that these sequences are not necessary for anchoring.

TMD sequences also act as topogenic signals for determining protein orientation in the membrane. The "positive-inside" rule states that protein topology is dictated by basic residues or net charge surrounding the first domain of the preproprotein (usually the signal/anchor sequence) to cross the membrane (von Heijne & Gavel, 1988; Hartmann et al., 1989; Boyd & Beckwith, 1990; von Heijne, 1989). The insulin preproreceptor signal/anchor sequence MGTGG*RR* GAAAAPLLVAVAALLLGAAG is followed directly by the amino terminus of the α-subunit *H*LYPG*E*VCPGM-*D*IRN... (membrane-spanning residues are underlined; charged residues are italicized) (Figure 2). Therefore, the positive-inside rule correctly predicts the surface orientation of the mature, wild-type insulin receptor. In the present study we have altered the positions of basic residues surrounding the second membrane-spanning sequence of the insulin preproreceptor (the stop-transfer sequence or TMD), which is the only membrane-spanning domain of the mature receptor. Neither neutralization of charge at the cytoplasmic surface (+exo/cyt), switching placement to opposite side of the TMD (++++exo/cyt), nor placement at both surfaces (++++exo/+++cyt) influenced holoreceptor topology. Even inverting the entire TMD including basic residues did not effect protein topology. These results are consistent with the positive-inside rule in that the signal/anchor sequence and not the stop-transfer sequence should determine topology. Presumably, by the time that the stop-transfer sequence is inserted into the ER membrane, topology has already been fixed by the signal/anchor sequence.

Results with the flip receptor clearly demonstrate that altering the TMD influences insulin proreceptor processing. The pathway for normal insulin receptor biosynthesis has been mapped previously in cultured lymphocytes (Hedo et al., 1983) and 3T3-L1 cells (Olson et al., 1988). Protein translation, cotranslational core glycosylations, preproreceptor processing, and certain disulfide isomerizations occur in the ER. Disulfide-mediated proreceptor dimerization and attachment of additional oligosaccharides occur in the *cis* Golgi, while oligosaccharide maturation and proteolytic processing of the proreceptor dimer into the mature $\alpha_2\beta_2$ holoreceptor occur in the *trans* Golgi or a later compartment. Our studies with transfected CHO cells fit this general scheme. The time course for biosynthesis and maturation of wild-type, +exo/cyt, and ++++exo/cyt receptors in CHO cells was similar to related events in the other cell types. Maturation was delayed for the flip receptor, however, judging by the amount of uncleaved propreceptor present at steady-state (over 90% vs 7% for wild-type). Similar amounts of the flip and wild-type proreceptors were synthesized, but proteolytic processing for the flip proreceptor was delayed. No uncleaved proreceptor forms were found at the cell surface, suggesting a block in intracellular transport, and the bulk of flip receptor immunoreactivity localized to the ER vs the cell surface for wild-type receptors.

A decreased rate of proteolytic processing between α- and β-subunits and flip proreceptor accumulation in the ER can both result from a reduced rate of release from the ER. As the ER lacks the necessary processing enzymes, proreceptor accumulates and reduced levels of mature receptor are observed at the cell surface. Therefore, TMD inversion—a change predicted to alter TMD homodimerization—caused retention of the receptor within the ER. ER retention was not observed for the other mutated receptors in this study (+exo/cyt, ++++exo/cyt) or following replacement of the entire insulin receptor TM with the analogous domains of the PDGF or neu/erbB2 receptors (Yamada et al., 1992; Cheatham et al., 1993). However, a Val→Asp substitution within the insulin receptor TMD also retards ER transfer (Yamada et al., 1992), although not to the degree observed for the flip receptor. These results suggest that a correct TMD sequence, even a heterologous tyrosine kinase TMD sequence, and not the presence or absence of flanking basic residues, signals ER release. Mutations that destabilize TMD homodimerization appear to block ER release. These

findings are consistent with the observations for T-cell and FC receptors suggesting that proper oligomeric assembly is required for transport from the ER to the Golgi (Bonifacino et al., 1990a,b; Manolios et al., 1990; Williams et al., 1990; Kurosaki et al., 1991; Lankford et al., 1993). Thus TMD interactions are necessary for T-cell and FC receptor oligomer assembly, and a related requirement may be necessary for assembly of insulin proreceptors and receptor maturation.

Although most of the flip receptor was retained in the ER and ultimately degraded, at steady-state ≈10% of total cellular immunoreactive receptor protein was present at the cell surface as a processed $\alpha_2\beta_2$ holoreceptor, allowing us to test flip receptor function. The assembled flip $\alpha_2\beta_2$ receptor bound insulin with normal affinity, but it failed to transmit the insulin binding signal to the intracellular kinase domain. Recognition of the flip receptor by several conformation-sensitive antibodies and the insulin binding studies suggested that significant portions of the extracellular receptor were properly folded. We previously showed that tryptic proteolysis provided an alternative method for activating the insulin receptor, by releasing the kinase domain from the inhibitory control of the extracellular domain (Shoelson et al., 1988). Trypsin has a similar effect with the flip receptor to demonstrate that the kinase domain is folded properly and can be activated. Therefore, functions at both sides of the membrane are intact, although the signaling connection between insulin binding and kinase domains of the flip receptor was lost. These findings, in conjunction with our previous studies (Yamada et al., 1992; Cheatham et al., 1993), suggest that TMD interactions are both necessary and sufficient for insulin-stimulated receptor activation. This unifying model for the activation of the insulin receptor, and presumably additional tyrosine kinase receptors as well, suggests that mutations which promote TMD dimerization activate the kinase, whereas mutations which abrogate TMD dimerization inhibit both ER release and kinase activation. Further tests of this model are underway.

REFERENCES

Bargmann, C. I., & Weinberg, R. A. (1988) *EMBO J. 7*, 2043.

Bargmann, C. I., Hung, M. C., & Weinberg, R. A. (1986) *Cell 45*, 649.

Boni-Schnetzler, M., Kaligian, A., DelVecchio, R., & Pilch, P. F. (1988) *J. Biol. Chem. 263*, 6822.

Bonifacino, J. S., Cosson, P., & Klausner, R. D. (1990a) *Cell 63*, 503.

Bonifacino, J. S., Suzuki, C. K., & Klausner, R. D. (1990b) *Science 247*, 79.

Boyd, D., & Beckwith, J. (1990) *Cell 62*, 1031.

Cao, H., Bangalore, L., Bormann, B. J., & Stern, D. F. (1992) *EMBO J. 11*, 923.

Cheatham, B., Shoelson, S. E., Yamada, K., Goncalves, E., & Kahn, C. R. (1993) *Proc. Natl. Acad. Sci. U.S.A. 90*, 7336.

Chou, P. Y., & Fasman, G. D. (1978) *Annu. Rev. Biochem. 47*, 251.

Downward, J., Yarden, Y., Mayes, E., Scrace, G., Totty, N., Stockwell, P., Ullrich, A., Schlessinger, J., & Waterfield, M. D. (1984) *Nature 307*, 521.

Ellis, L., Morgan, D. O., Clauser, E., Roth, R. A., & Rutter, W. J. (1987) *Mol. Endocrinol. 1*, 15.

Fratalli, A. L., Treadway, J. L., & Pessin, J. E. (1992) *J. Biol. Chem. 267*, 19521.

Goncalves, E., Yamada, K., Thatte, H. S., Backer, J. M., Golan, D. E., Kahn, C. R., & Shoelson, S. E. (1993) *Proc. Natl. Acad. Sci. U.S.A. 90*, 5762.

Gullick, W. J., Bottomley, A. C., Lofts, F. J., Doak, D. G., Mulvey, D., Newman, R., Crumpton, M. J., Sternberg, M. J. E., & Campbell, I. D. (1992) *EMBO J. 11*, 43.

Harbury, P. B., Zhang, T., Kim, P. S., & Alber, T. (1993) *Science 262*, 1401.

Hartmann, E., Rapoport, T. A., & Lodish, H. F. (1989) *Proc. Natl. Acad. Sci. U.S.A. 86*, 5786.

Hedo, J. A., Kahn, C. R., Hayoshi, M., Yamada, K. M., & Kasuga, M. (1983) *J. Biol. Chem. 258*, 10020.

King, C. R., Kraus, M. H., & Aaronson, S. A. (1985) *Science 229*, 974.

Kurosaki, T., Gander, I., & Ravetch, J. V. (1991) *Proc. Natl. Acad. Sci. U.S.A. 88*, 3837.

Lankford, S. P., Cosson, P., Bonifacino, J. S., & Klausner, R. D. (1993) *J. Biol. Chem. 268*, 4814.

Manolios, N., Bonifacino, J. S., & Klausner, R. D. (1990) *Science 249*, 274.

Olson, T. S., Bamberger, M. J., & Lane, M. D. (1988) *J. Biol. Chem. 263*, 7342.

Richardson, J. S., & Richardson, D. C. (1988) *Science 240*, 1648.

Shoelson, S. E., White, M. F., & Kahn, C. R. (1988) *J. Biol. Chem. 263*, 4852.

Shoelson, S. E., Lu, Z., Parlautan, L., Lynch, C. S., & Weiss, M. A. (1992) *Biochemistry 31*, 1757.

Sternberg, M. J. E., & Gullick, W. J. (1989) *Nature 339*, 587.

Sweet, L. J., Morrison, B. D., Wilden, P. A., & Pessin, J. E. (1987) *J. Biol. Chem. 262*, 16730.

Treadway, J. L., Morrison, B. D., Soos, M. A., Siddle, K., Olefsky, J., Ullrich, A., McClain, D. A., & Pessin, J. E. (1991) *Proc. Natl. Acad. Sci. U.S.A. 88*, 214.

Ullrich, A., & Schlessinger, J. (1990) *Cell 61*, 203.

Ullrich, A., Bell, J. R., Chen, E. Y., Herrera, R., Petruzzelli, L. M., Dull, T. J., Gray, A., Coussens, L., Liao, Y.-C., Tsubokawa, M., Mason, A., Seeburg, P. H., Grunfeld, C., Rosen, O. M., & Ramachandran, J. (1985) *Nature 313*, 756.

von Heijne, G. (1989) *Nature 341*, 456.

von Heijne, G., & Gavel, Y. (1988) *Eur. J. Biochem. 174*, 671.

Weiner, D. B., Liu, J., Cohen, J. A., Williams, W. V., Greene, M. I. (1989) *Nature 339*, 230.

Williams, G. T., Venkitaraman, A. R., Gilmore, D. J., & Neuberger, M. S. (1990) *J. Exp. Med. 171*, 947.

Yamada, K., Goncalves, E., Kahn, C. R., & Shoelson, S. E. (1992) *J. Biol. Chem. 267*, 12452.

BI942056+